

Submillimeter-wave spectral response of twin-slot antennas coupled to hot electron bolometers

R.A. Wyss, A. Neto, W.R. McGrath, B. Bumble, H. LeDuc

*Center for Space Microelectronics Technology, Jet Propulsion Laboratory,
California Institute of Technology, Pasadena, CA 91109*

ABSTRACT

The spectral response of quasioptical hot-electron bolometer (HEB) mixers has been measured with a Fourier transform spectrometer. In this study we have measured mixers with a wide range of twin-slot antennas with slot lengths ranging from 26 μm up to 152 μm . For all designs, the measured center of the direct detection response was lower than predictions based on a Method-of-Moment (MoM) calculation of a simplified mixer embedding circuit model. This model took into account the slot antennas and the coplanar waveguide embedding circuit, but not the parasitic effects associated with the couplings of these elements or the HEB device geometry. The frequency shift becomes particularly significant at frequencies beyond 1 THz, and is in excess of 20% for the smallest antennas. Such large shifts reduce the radiation coupling efficiency by more than 3 dB, and hence increase the mixer noise temperature unnecessarily. To resolve the discrepancy between the observations and the model predictions we have introduced two essential refinements into the MoM model which account for (1) the coplanar waveguide (CPW) to slot-antenna transition, and (2) the inductance associated with the effective narrowing of the CPW center lead as represented by the HEB bridge. The results of these model refinements prove to have a small effect on the real-part of the embedding impedance but a dramatic effect on the imaginary-part. In fact, the inductance of the narrow microbridge dominates the estimated frequency shift. Thus we find that properly modeling the entire embedding circuit and the device geometry leads to a better agreement with the measured results.

Introduction

Previously reported results by Karasik *et al.*^[1] have shown the center frequency of the peak direct detection response of HEB mixers employing a twin slot-antenna and CPW embedding circuit to be lower than anticipated by up to 20%. The magnitude of the shift is especially dramatic for antenna designs at the very highest frequencies, where HEB mixers have shown their most competitive performance. For example, a twin-slot antenna design, which has been scaled from a 600 GHz design to 2.5 THz, has a peak response at about 2 THz^[2]. That is a shift of 500 GHz. Several explanations have been

proposed, such as the effects of finite metal thickness^[3], limitations of scale-model predictions when extrapolating into the THz frequency region, and parasitics associated with transitions between circuit elements.

In this paper we will report the results of an extensive experimental study of HEB mixers with six different twin-slot antenna designs. The spectral response and hence the center frequency is measured with a Fourier-transform spectrometer. Method-of-Moments (MoM) calculations of both a simplified model^[4] and a more complete model of the mixer embedding circuit will be compared to the measured results. Understanding the limitations of the circuit models and hence causes of the frequency shift will be critical to designing HEB mixers having a peak response at a desired frequency. Ultimately, this will make possible the design of high-frequency heterodyne mixers that obtain the best possible mixer noise temperatures.

Experiment

Figure 1(a) shows an SEM photograph of our 2 THz HEB mixer. The submicron-sized HEB device (i.e. “microbridge” in the figure) is connected to the twin slot-antennas by CPW transmission line^[5]. On the the right a flared-shaped center conductor is used as the first element of the intermediate frequency (IF) filter structure (a total of six high and low impedance sections were used).

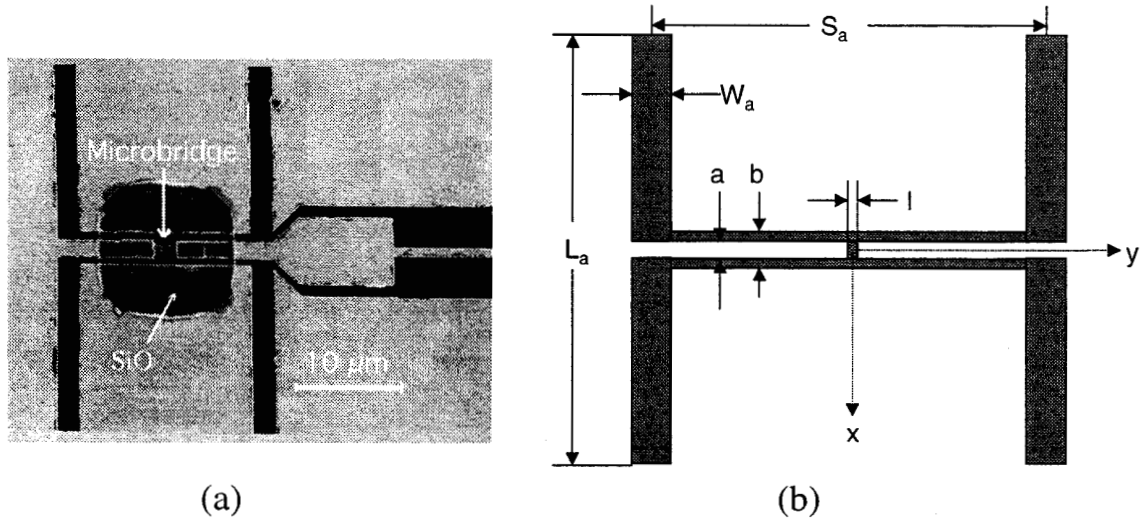


FIG. 1.(a) Photograph of HEB antenna structure. The superconducting bridge is located at the center and coupled to the twin-slot antenna via CPWs. (b) Schematic layout of physical structure used in the simulation with the relevant dimensions defined.

Figure 1(b) defines the relevant parameters for the model we will present in the second half of the paper. The length of the gap between the CPW terminals is l and the width of the microbridge is w (not shown in the figure).

The direct detection response of the HEB devices was measured using a Bruker IFS120HR Fourier-transform spectrometer. The spectral resolution during the runs was set to 1 cm^{-1} (3 GHz). A mylar beamsplitter thickness of $50 \mu\text{m}$ was used for the $152 \mu\text{m}$ -long slot antenna in order to obtain sufficient signal-to-noise at frequencies below about 1 THz. All the higher frequency twin-slot antennas were measured using a $23 \mu\text{m}$ -thick Mylar beamsplitter which yielded sufficient signal for the range 1 – 3 THz.

For the spectral measurements, the HEB was either constant-current or constant-voltage biased. No difference in the output spectrum was observed for the two different bias schemes. The method used during the measurement was chosen based on better bias stability and lower noise in the output signal. The HEB was operated in a 4 K LHe vacuum-cryostat with an optical access port. The device temperature was set to the transition edge temperature at $\approx 6 \text{ K}$. To facilitate stable temperature and minimize the LHe boil-off rate, the mixer block inside the cryostat was mounted on an aluminum post. By applying a dc bias voltage to a heater resistor affixed to the mixer block, the temperature of the block could be controlled and held constant to a precision of $\pm 10 \text{ mK}$. The bias point and the mixer block temperature was chosen to maximize the interferogram signal.

Spectral Response Measurement

Table 1 summarizes the properties of the seven devices measured. We have denoted the antenna design with two numbers: the intended center frequency of the design, ν_c , and the length of the slots, L_a .

Table 1. Mixer characteristics.

Mixer	Antenna Design $\nu_c [\text{THz}]/L_a [\mu\text{m}]$	w [μm]	l [μm]	$R_{\text{Device}}^{\ddagger}$ T = 295K	$R_{\text{Device}}^{\ddagger}$ T = 4K	I_c^{\dagger} [μA]	T_{meas}^{\S} [K]
1	2.5/26	0.1	0.2	34	15	240/200	5.03
2	2.5/33	0.1	0.1	-	18	185/171	6.1
3	2.5/36.5	0.1	0.1	-	18	225/107	6.4
4	2.5/36.5	0.15	0.3	-	25	300/120	6.7
5	1.65/44	0.1	0.2	100	46	78/56	5.5
6	1.9/48	0.15	0.3	81	25	172/100	5.68
7	0.6/152	0.15	0.15	75	32	125/50	4.88

$^{\ddagger}R_{\text{Device}}$ is the HEB device DC resistance

$^{\dagger}I_c$ is the device critical current

$^{\S}T_{\text{meas}}$ is the transition temperature

In Fig. 2 we show the spectral response for mixer 1 and 7, which is representative of the data sets. The spectra have been normalized to the Mylar beamsplitter transmission which was measured using a pyroelectric detector. The response of this reference detector is assumed to be independent of frequency in the range of interest. The measured bandwidths are typically on the order of 50%, increasing slightly for the

highest frequency mixers with the shortest antenna slots. The additional peaks around 1.8 THz for the 152 μm twin-slot antenna are due to a low signal level when using a 50 μm Mylar beamsplitter. The measurements typically required the averaging of 300 spectra having a resolution of 1 cm^{-1} to achieve the signal-to-noise level displayed in fig. 2. A Gaussian fit was used to find the center and FWHM of the curves.

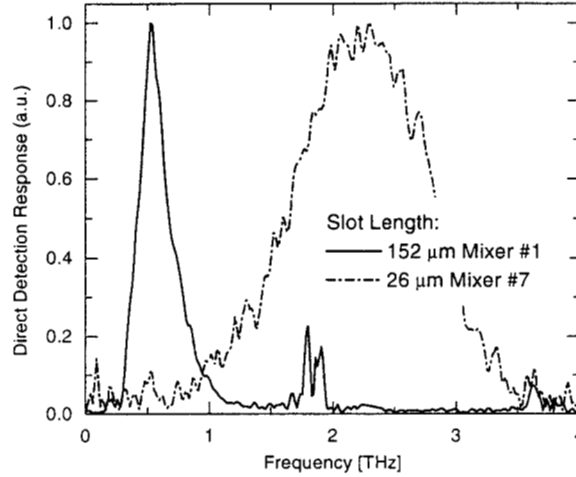


FIG. 2. FTS direct detection response of two mixers (#1 and #7) having slot-antenna lengths equal to 152 μm and 26 μm , respectively.

Table 2 gives a summary of the antenna parameters for each mixer and the measured center frequency. The circuits (CPW lines and slots) are approximately scaled for each frequency, although for the smallest ones, the device fabrication process limited the smallest dimensions of the CPW. Two types of transitions between the slot and the IF-filter were implemented – an abrupt and a tapered transition. The influence on the center frequency and bandwidth is not exactly understood, but based on the current data their influence is found to be secondary. The last column shows the predicted center frequency based on a MoM calculation when treating the twin-slot and CPW as separate elements (that is, no interaction between the two is included). The calculation of the antenna impedance was done using a Fortran code obtained from G. Chattopadhyah^[6] (similar calculations have been published by several groups). This antenna impedance is then transformed through the length of the CPW line to the device terminals. The coupling efficiency, η , to the HEB device is found using the following well-known impedance-mismatch expression:

$$\eta = 1 - \left| \frac{Z_{\text{HEB}} - 2Z_1}{Z_{\text{HEB}} + 2Z_1} \right|^2,$$

where Z_{HEB} is the device impedance (assumed to be real) and Z_1 is the impedance looking into each terminal. Since we assume that the HEB RF impedance is real, the peak response occurs when the imaginary part of the embedded circuit impedance is zero.

Table 2. Antenna parameters, measured and calculated center frequencies.

Mixer	L_a (μm)	W_a (μm)	S_a (μm)	a (μm)	b (μm)	Z_{cpw} (Ω)	IF-Filter	ν_c Measured (THz)	ν_c Calculated (THz)
1	26	3	19	3	4	35.6	abrupt	2.22	2.98
2	33	3	19	3	4	35.6	abrupt	2.19	2.60
3	36.5	2	19	2	3	39.4	tapered	2.02	2.31
4	36.5	2	19	2	3	39.4	tapered	2.01	2.31
5	44	4	25	4.5	6	35.6	abrupt	1.60	2.01
6	48	2.6	25	3	4.4	38.6	tapered	1.71	1.76
7	152	8.3	79.2	8	11	36.4	tapered	0.54	0.57

The three smallest designs are very similar. The intention was to progressively shorten the slot length, and by way of this empirical method to achieve a center frequency of 2.5 THz. This approach worked initially: shortening the slots from 36.5 μm to 33 μm did increase the resonant frequency by the expected 10% or 200 GHz. Further reducing the slot length to 26 μm , however, did not shift the peak response by a proportionate amount. In fact, the shift was as little as 30 GHz. It became clear that some other important physical effect was playing a significant role in determining the frequency response besides just the slot antenna length. The largest discrepancy between the observation and the calculated peak response is for the smallest antenna design (a shift of about 25%).

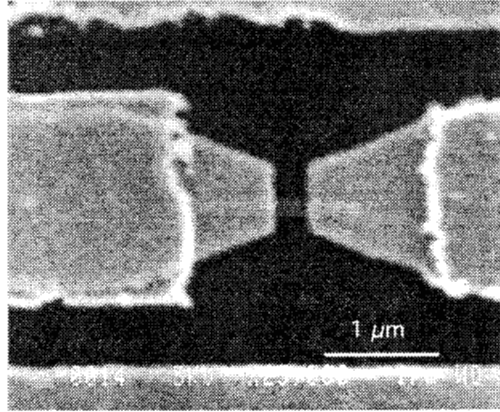


FIG. 3. Photograph of HEB device center region. Terminal connection design is tapered over a distance of about 1 μm with a flare angle of 45°. The bridge is the faint horizontal bar connecting the two terminals. For the CWP shown, the center conductor width is 2 μm and the gaps are 0.5 μm .

Discussion

The discrepancy between the theoretical predictions and the mixer direct spectral response made clear that our model is incomplete. In this section we present an improved model of the slot antenna/CPW/HEB-microbridge and show that significantly better predictions are possible. The model predicts the general trends that will drive the next

generation mixer designs and helps to better predict the location of the HEB mixer peak response.

The first improvement is to include the transition between the CPW line and the slot antennas. The fringing fields at these junctions add a parasitic reactance to the circuit. The second refinement will be to take account of the reactance (inductance) of the very narrow HEB bridge. Figure 3 shows an SEM photograph of the center region of the embedding circuit. The microbridge is the faint gray horizontal stripe connecting the two terminals. The tapered transition region was introduced to ease alignment during fabrication. The analysis of this geometry has been performed using a previously developed MoM code^[7]. This code was written to take account of the reactive energy of the bend and the narrowing of the center conductor.

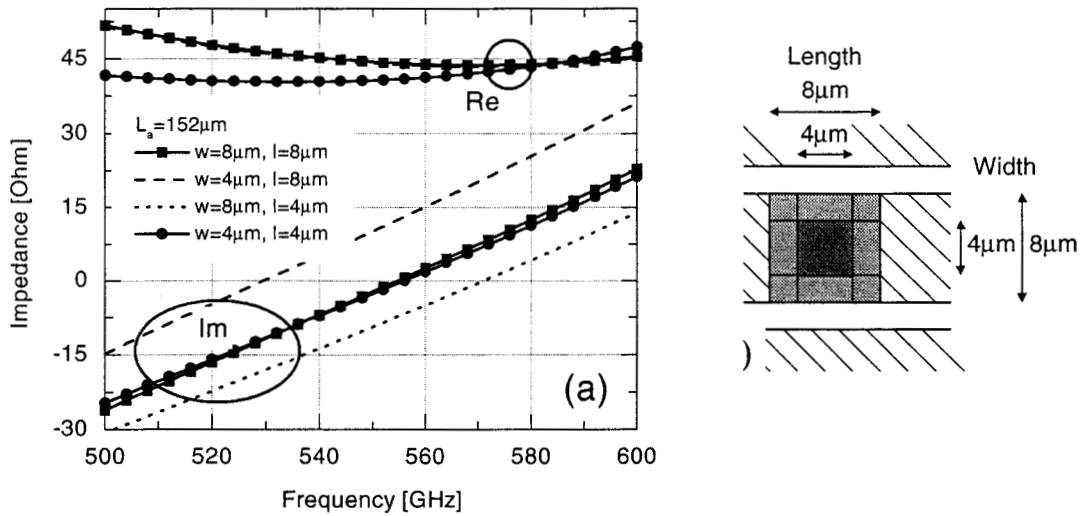


FIG. 4. Dependence of embedding impedance on frequency for several different microbridge sizes. The resonance frequency occurs where the imaginary part passes through zero. (b) The microbridge dimensions used in the simulation.

In Fig. 4 we show the results of the calculation for the mixer with $152 \mu\text{m}$ -long slot-antennas. To illustrate the general behavior we varied the size of the HEB microbridge while keeping the CPW and slot dimensions fixed. For the largest microbridge ($8\text{-by-}8 \mu\text{m}^2$) the predicted peak response (i.e. where the imaginary part of the impedance crosses zero) is 555 GHz , which is very close to the measured 554 GHz . When the width of the source region is decreased to $4 \mu\text{m}$, the inductance due to the reduced width of the bridge increases and the imaginary impedance increases by about 15Ω at 555 GHz . Since the frequency dependence of the imaginary impedance is relatively flat, this leads to a large shift in the zero crossing and, hence, the location of the peak coupled power. A shift in the opposite direction can be accomplished by decreasing the length of the bridge and keeping the width constant. This predominantly affects the capacitive reactance of the gap between the center leads of the CPW. Finally, the location of the peak response

is unaffected when keeping the length-to-width ratio constant (4-by-4 μm^2). The real part of the impedance is barely influenced by the change of the device geometry.

The above example clearly demonstrates the strong influence of the HEB device geometry on the predicted location of the peak. In the next example we have calculated the center frequency of the mixer with a 26 μm twin-slot antenna structure. Since the computational burden on our straightforward MoM implementation is quite large, we employed the following constraints: (1) use a 1 μm resolution ($\lambda_0/110$) which results in ~ 200 piecewise sinusoidal (PWS) functions; (2) set the length of the bridge to 2 μm ; and (3) vary the bridge width from 3 μm to 1 μm . Figure 5 shows a summary of the results.

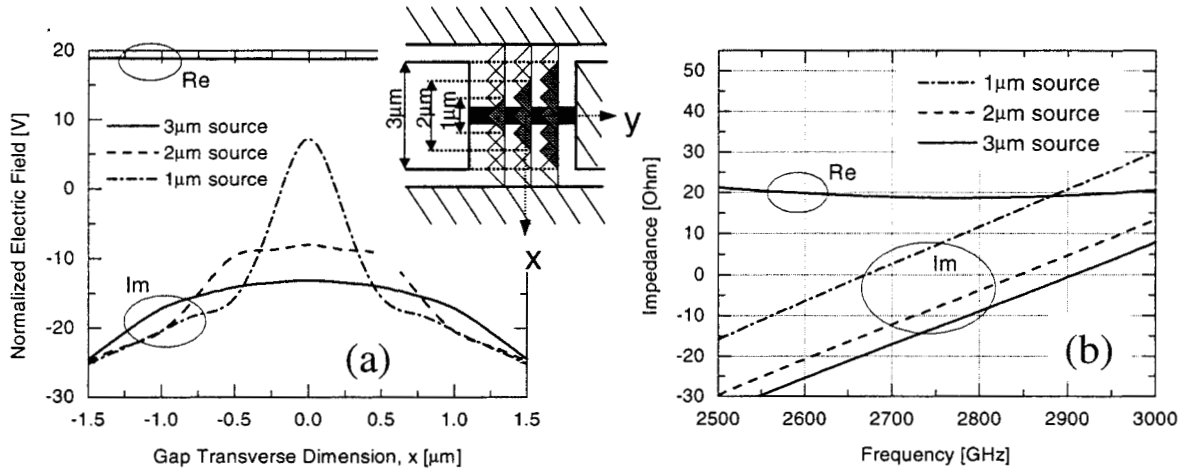


FIG. 5.(a) Real and imaginary amplitude of the normalized electric field along the x -direction at 2.75 THz. Inset shows the orientation of the seven PWS functions in the device region. (b) Shift in peak response due to reducing the device width. The gap length is kept constant and sufficiently long to minimize the influence of any capacitive induced effects.

Figure 5(b) illustrates that the real part of the electric field (i.e. magnetic current) is completely unaffected by the bridge width. The imaginary part, however, depends dramatically on the transverse dimension. For the 3 μm -wide bridge (solid line) the imaginary part is slowly varying as a function in the gap's transverse direction. For the 2 μm case (dashed line) a more significant growth of about 6 Ω is observed at the center of the bridge. As the bridge is further reduced to 1 μm (dash-dotted line), the increase amounts to 25 Ω , which is of the same order of magnitude as the real part of the impedance. The fact that the electric field tends to be peaked in the surrounding of the microbridge can easily be explained. As the bolometer region becomes small in terms of wavelength, the concentrated current flow through the bridge tends to radiate a Hankel function shaped electric field^[7]. The singularity of this field is logarithmic as the width approaches zero. Thus, we expect a logarithmic growth of the imaginary part of the electric field at the center. This qualitative behavior was observed at all frequencies investigated, and the impact of this behavior is quantified in Fig.5(b).

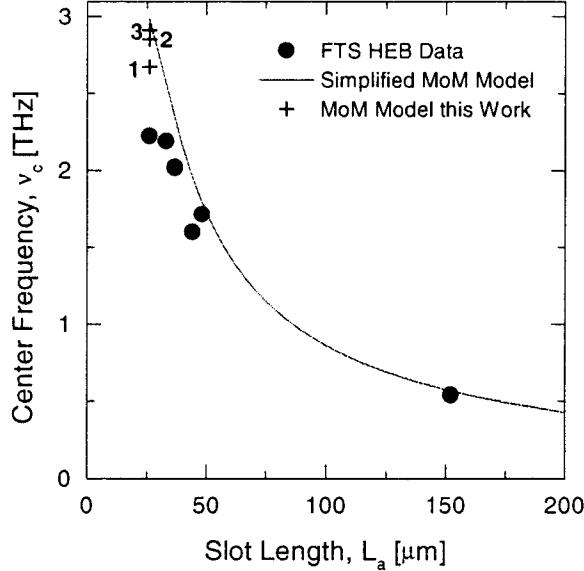


FIG. 6. Summary of experimental data from mixers with six different length twin-slot antenna designs (•). Center frequency of simplified model predicted using G. Chattopadhyah's code^[6] (solid line). Results of model for the 26 μm twin-slot antenna including parasitics (+). The HEB bridge is either 1, 2 or 3 μm wide.

The zero Ohm level (resonance) is crossed at 2.91 THz as predicted earlier (see Table 2). In this case the HEB device is as wide as the CPW center conductor, and so there is no additional inductance associated with it. However, the resonance frequency is about 3% lower than the 3 THz, which is predicted for the slots and CPW without any interaction. Thus this small shift (3.0 to 2.91 THz) is due to the reactance of the junction of the CPW line with the slot antenna. When a 2 μm -wide device is introduced, a jump of 6 Ω is observed. Associated with this augmented reactive energy is a shift downward of the resonating frequency to 2.85 THz. A further shift to 2.67 THz follows upon decreasing the device width to 1 μm . It is evident that a further reduction downward in resonating frequency would follow when one further reduces the width of the microbridge. The example has shown that the predominant source of the downward shift is due to the inductive reactance associated with the bolometer itself, while the shift due to the CPW-to-slot junction is small by comparison. We expect to be able to account for the observed 25-30% shift when introducing the actual width of 0.1 μm of the bolometer. Of course, the final calculation will have to take account of the much shorter bridge length, between 0.1 to 0.3 μm . The added capacitance will compensate and shift upwards the resonance frequency somewhat. This “gap capacitance” can potentially be used to provide a low-Q (i.e. broadband) tuning of the device inductance. In Fig. 6 we have summarized the experimental results and the predictions obtained from the two models used to explain the data.

Taking into account the constriction of the RF current caused by the narrow width of the HEB device proved to significantly influence the predicted center frequency. More

importantly, using the refined model made it possible to identify the key source of discrepancy between the observed behavior and predictions. Especially at the highest frequencies, the inductance of the microbridge causes the large frequency shift.

Conclusion

This paper has presented FTS measurements of THz HEB mixers with a large range of twin slot-antenna designs. A discrepancy had been noted in the actual location of the peak response and predictions based on MoM calculations using a simple circuit model. Refinements of this model, including the CPW-to-slot junction and the narrow width of the HEB device, lead to both an understanding of the causes for the discrepancy and better predictions. The realization that the HEB bridge inductance is responsible for a dominant part of the shift is a breakthrough.

Although further refinements in the model description – possible analytical models – are required to accurately describe the extremely short and narrow bridge correctly, this paper makes a significant contribution in identifying the key elements responsible for the observed downward frequency shifts.

Acknowledgments

This research was performed in the Center for Space Microelectronics Technology, Jet Propulsion Laboratory, California Institute of Technology, and was sponsored by the National Aeronautics and Space Administration, Office of Space Science.

References

- [1] B.S. Karasik, M.C. Gaidis, W.R. McGrath, B.Bumble, and H.G. LeDuc, "A low-noise 2.5 THz superconductive Nb hot-electron mixer," *IEEE Trans. Appl. Supercond.* 7 (2), 3580 (1997).
- [2] R.A. Wyss, "Noise and bandwidth measurements of diffusion-cooled Nb hot-electron bolometer mixers at frequencies above the superconductive energy gap" *Proc. of the 10th Int. Symp. on Space THz Tech.*, University of Virginia, Charlottesville, VA (1999).
- [3] W.F.M. Ganzevles, T.M. Klapwijk, L.R. Swart, J.R. Gao, and P.A.J. de Korte, "Direct response of twin slot antenna coupled hot-electron bolometer mixers designed for 2.5 THz radiation detection", submitted to *Appl. Phys. Lett.* (12/15/99).
- [4] J. Zmuidzinas and H.G. Leduc, "Quasi-optical slot antenna SIS mixers", *IEEE Trans. Microwave Theory Tech.*, vol. 40 (9), pp. 1797-1804 (1992).

- [5] B. Bumble and H.G. LeDuc, "Fabrication of a diffusion cooled superconducting hot electron bolometer for THz mixing applications," *IEEE Trans. Appl. Supercond.* **7** (2), 3560 (1997).
- [6] Fortran code calculating the impedance of a coupled twin-slot antenna was obtained from Goutam Chattopadhyah. Computational approach described in Ref. 4.
- [7] A. Neto, P.J.I. de Magt, and S. Maci, "Full wave analysis of slot antennas excited by coplanar waveguides", preprint, (2000).